Supplement of Atmos. Chem. Phys., 21, 853–874, 2021
https://doi.org/10.5194/acp-21-853-2021-supplement

Atmospheric Chemistry and Physics
Open Access

Supplement of

Effective radiative forcing from emissions of reactive gases and aerosols – a multi-model comparison

Gillian D. Thornhill et al.

Correspondence to: Gillian D. Thornhill (g.thornhill@reading.ac.uk)

The table of models used in the paper with information on resolution and aerosol and chemistry modules.

Table S 1 Table of model properties, aerosol schemes, and chemistry (SU = sulphate; OA = organic aerosol; BC = black carbon; DU = dust; SS = sea salt; NO3 =nitrate)

Earth System Model (component models)	Resolution	Description of aerosol module	References
IPSL-CM6A-LR (LMDz, INCA)	1.25°(lat) x 2.5°(lon) 79 vertical levels LMDzORINCA Two	LMDzORINCA Two-moment (mass and number) aerosol scheme with 5 lognormal modes. The IPSLCM6A-LR-INCA model used for this analysis has interactive aerosols but a limited gas-phase model. Aerosol scheme is based a sectional approach with to represent the size distribution of dust, Sea- salt (which has an additional super-coarse mode to model largest emission of spray-salt aerosols), BC, NH4, NO3, SO4, SO2 and OA with a combination of accumulation and coarse log-normal modes with both, soluble and insoluble, treated as independent modes. DMS emissions are prescribed and not interactively calculated. BC is modelled as internally mixed with sulphate (Wang et al., 2016), where the refractive index is relies on Garnet-Maxwell method. Its emissions are derived from inventories. A new dust refractive index is implemented (Di Biagio et al., 2019). Well mixed trace gases concentrations/emissions are forced with AMIP/CMIP6 datasets (Lurton et al., 2020) ozone by (Checa-Garcia et al., 2018) and solar forcing by (Matthes et al., 2017) Components included: SU, BC, OA, SS, DU, NO3	(Balkanski et al., 2010) (Hauglustaine et al., 2014)

UKESM11 (HadGEM3, UKCA, JULES)	1.25°(lat) x 1.88°(lon) 85 vertical levels	UKCA contains the GLOMAP-mode aerosol microphysics scheme Two-moment (mass and number) aerosol scheme with 5 lognormal modes (nucleation soluble, Aitken soluble, Aitken insoluble, accumulation soluble, coarse soluble) Components included: SU, BC, OA, SS, DU* *Dust component tracked independently in six size bins UKCA contains a stratosphere-troposphere chemistry scheme, consisting of 84 tracers, 81 species, 199 bimolecular reactions, 25 uni- or termolecular reactions, 5 heterogeneous, 3 aqueous phase reactions, and 59 photolytic reactions. Secondary aerosol formation of sulphate and secondary organic aerosol is determined by the interactive oxidants. The UKCA aerosol scheme, called GLOMAP-mode, is a two-moment scheme for the simulation of tropospheric black carbon (BC), organic carbon (OC), SO_4, and sea salt. Dust is modelled independently using the bin scheme of Woodward (2001). The UKCA chemistry and aerosol schemes are coupled such that the secondary aerosol (SO_4, OA) formation rates depend on oxidants from the stratosphere-troposphere chemistry scheme. Aerosol particles are activated into cloud droplets using the activation scheme of Abdul-Razzak and Ghan (2000) which is dependent on aerosol size distribution, aerosol composition, and meteorological conditions. Changes in CDNC affect cloud droplet effective radius ((Jones et al., 2001) and the auto conversion of cloud liquid water in to rain water (Khairoutdinov and Kogan, 2000), which both influence cloud albedo. Stratospheric aerosols (aerosol optical depth and surface area density) are prescribed in the model (Sellar et al., 2019b).	(Sellar et al.) (Williams et al., 2018) (Walters et al., 2019) (Kuhlbrodt et al., 2018) GLOMAP-mode by (Mann et al., 2010) (Mulcahy et al., 2018) (Morgenstern et al., 2009) (O'Connor et al., 2014) (Archibald et al., 2020;Sellar et al., 2020;Mulcahy et al., 2020)

CNRM-ESM2-1 (ARPEGEClimatv6.3, ISBA-CTRIP, TACTIC, REPROBUS, PISCES)	1.4°(lat) x 1.4°(lon) 91 vertical levels	Aerosols: TACTIC_v2 tropospheric aerosol bin scheme. 12 bins in total for SU, BC, OA, SS, DU, with 3 bins for SS, and 3 bins for DD. REPROBUS_v2 stratospheric chemistry scheme with 63 variables, 44 transported by the model large-scale transport scheme, and 168 chemical reactions, among which 39 photolysis and 9 heterogeneous reactions	(Séférian et al., 2016;Michou et al., 2015) (Séférian et al.) 2019 Michou et al 2019 Model description website: http://www.umrcnrm. fr/cmip6/spip.ph p?article10
NorESM2 CAM6-Nor, CLM5)	1.9°(lat) x 2.5°(lon) 32 vertical levels	OsloAero6 Production-tagged aerosol module with background lognormal modes (Aitken, accumulation, coarse). Process tracers can alter the shape and composition of the initially lognormal background modes to generate mixtures. OsloAero6 aerosol module which contains some slight updates since (Kirkevåg et al., 2018) describes the formation and evolution of BC, OC, SO_4, dust, sea-salt and SOA. There is a limited gas-phase chemistry describing the oxidation of the aerosol precursors DMS, SO_2, isoprene, and monoterpenes. Oxidant fields of OH, HO_2, NO_3 and O_3 are prescribed climatological fields. As there is no ozone chemistry in the model, prescribed monthly-varying ozone fields are used for the radiation. Components included: SU, BC, OA, SS, DU	(Kirkevåg et al., 2018)

MRI-ESM2	MRI-AGCM3.5: TL159; 320 x 160 lon/lat, MASINGAR mk-2r4c: TL95; 192 x 96 lon/lat, MRI-CCM2.1: T42; 128 x 64 lon/lat, with 80 vertical levels	MASINGAR mk-2r4c is an aerosol model that is a component of MRI-ESM2.0. MASINGAR mk-2r4c treats atmospheric aerosol physical and chemical processes (e.g., emission, transport, diffusion, chemical reactions, and dry and wet depositions). The size distributions of sea salt and mineral dust are divided into 10 discrete bins and those of other aerosols are represented by lognormal size distributions. Components included: SU, BC, OA, SS, DU	(Yukimoto et al., 2019) (Oshima et al., 2020)
MIROC6	1.4º (lat) x 1.4º (lon)	Spectral Radiation-Transport Model for Aerosol Species (SPRINTARS) predicts mass mixing ratios of the main tropospheric aerosols, and models aerosol-cloud interactions in which aerosols alter cloud microphysical properties and affect the radiation budget by acting as cloud condensation and ice nuclei. The SO_4, BC and OC aerosols are treated as externally mixed in this model. The CDNC and ice crystal number are used to calculate the aerosol indirect effect and cloud nucleation process Components included: SU, BC, OA, SS, DU	(Takemura et al., 2005;Watanabe et al., 2010;Takemura and Suzuki, 2019;Takemura, 2018;Tatebe et al., 2019)

BCC-ESM1 (BCC-AGCM3-Chem, BCC-AVIM2, MOM4-L40, SIS)	2.8125º (lat) x 2.8125º (lon) 26 vertical levels with top level at 2.914 hPa	The model prognoses mass distribution of five aerosol types including sulfate, dust, black carbon, organic carbon, and sea salt based on their emissions (and precursor emissions), chemical production for sulfate and secondary organics, dry and wet (rainout and washout) deposition, transport by advection, and dry and wet convection. It uses the BCC-AGCM3-Chem atmospheric chemistry model based on MOZART2 (Horowitz et al., 2003) It uses the BCC-AGCM3-Chem atmospheric chemistry model based on MOZART2 (Horowitz et al., 2003) which does not include stratospheric chemistry, so concentrations of O_3, CH_4, and N_2O at the top two model levels are the zonally and monthly values derived from the CMIP6 data package. Components included: SU, BC, OA, SS, DU Effects of aerosols on radiation, cloud, and precipitation are treated.	(Wu et al., 2020)

GFDL-ESM4	(C96 96x96 cells) 49 vertical levels	The model includes 56 prognostic (transported) tracers and 36 diagnostic (non-transported) chemical tracers, with 43 photolysis reactions, 190 gas-phase kinetic reactions, and 15 heterogeneous reactions. The tropospheric chemistry includes reactions for the NO_x-HO_x-O_x-CO-CH_4 system and oxidation schemes for other non-methane volatile organic compounds. The stratospheric chemistry accounts for the major ozone loss cycles (O_x, HO_x, NO_x, ClO_x, and BrO_x) and heterogeneous reactions on liquid and solid stratospheric aerosols as in Austin et al. (2013). The bulk aerosol scheme, including 18 transported aerosol tracers, is similar to that in AM4.0 (Zhao et al., 2018), with the following updates: (1) ammonium and nitrate aerosols are treated explicitly, with ISORROPIA (Fountoukis and Nenes, 2007) used to simulate the sulfate–nitrate–ammonia thermodynamic equilibrium; (2) oxidation of sulfur dioxide and dimethyl sulfide to produce sulfate aerosol is driven by the gas-phase oxidant concentrations (OH, H_2O_2, and O_3) and cloud pH simulated by the online chemistry scheme, and (3) the rate of aging of black and organic carbon aerosols from hydrophobic to hydrophilic forms varies with calculated concentrations of hydroxyl radical (OH). Aerosol species, including sulfate, BC, organic aerosols, sea-salt, dust and nitrate are treated explicitly.	(Horowitz et al., 2020;Dunne et al., 2020)
GISS-E2-1 (p3 variant)	2° latitude by 2.5° in longitude 40 vertical layers surface to 0.1 hPa in	Aerosols and ozone are calculated prognostically using the One-Moment Aerosol (OMA). Aerosol scheme is coupled to the tropospheric chemistry scheme which includes inorganic chemistry of O_x, NO_x, HO_x, CO, and organic chemistry of CH_4 and higher hydrocarbons using the CBM4 scheme and the stratospheric chemistry scheme which includes chlorine and bromine chemistry together with polar stratospheric clouds.	(Bauer et al., 2020;Shindell et al., 2001;Shindell et al., 2003;Gery et al., 1989;Shindell et al., 2006)

CESM2-WACCM	0.9 (lat) x 1.25 (lon), 70 levels	Chemistry and aerosols for the troposphere, stratosphere, mesosphere and lower thermosphere are calculated interactively. It simulates 228 compounds, including the 4-mode Modal Aerosol Model (MAM4). This version of MAM4 is modified to allow for the simulation of stratospheric aerosols from volcanic eruptions (from their SO_2 emissions) and oxidation of OCS. The representation of secondary organic aerosols follows the Volatility Basis Set approach.	(Emmons et al., 2020;Danabasoghu, 2019;Danabasoglu, 2019;Gettelman et al., 2019;Tilmes et al., 2019) Mills et al., 2016)

(Table for European models updated from:

Crescendo Report Horizon 2020

H2020-SC5-2014 Advanced Earth-system models

(Grant Agreement 641816)

Coordinated Research in Earth Systems and Climate: Experiments, kNowledge, Dissemination and OutreachDeliverable D_6.2

S2 Tables of ERF and ERF_ts for all models analysed

By removing the adjustment due to the changes in the land surface temperature (as calculated from radiative kernels) we show the ERF_Ts for those models where the adjustment was available in the following table.

The tables below give the 1850-2014 ERF and the ERF_Ts calculated from the TOA flux differences for each model for each experiment.

Table S 2 ERFs and ERF_ts for the aerosols, including multi-model means with standard errors.

ERF	aer		BC		OC		SO2		NH3	
Wm^{-2}	ERF	ERF_ts	ERF	ERF_ts	ERF	ERF_ts	ERF	ERF_ts	ERF	ERF_ts
CNRM-ESM2	-0.74	-0.79	0.11	0.11	-0.17	-0.18	-0.75	-0.78		
UKESM1	-1.10	-1.15	0.37	0.36	-0.21	-0.23	-1.36	-1.41		
MRI-ESM2	-1.21	-1.24	0.25	0.27	-0.32	-0.32	-1.37	-1.42		
BCC-ESM1	-1.47	-1.54	0.21	0.21			-1.54	-1.62		

MIROC6	-1.01	-1.07	-0.21	-0.24	-0.23	-0.26	-0.64	-0.67		
NorESM2	-1.21	-1.21	0.30	0.30	-0.22	-0.23	-1.28	-1.29		
GFDL-ESM4	-0.70	-0.73								
GISS-E2-1	-0.90	-0.95	0.06	0.06	-0.44	-0.45	-0.62	-0.65	-0.08	
IPSL-INCA	-0.75		0.10		-0.15		-0.69		-0.06	
MultiModel Mean	-1.01	-1.09	0.15	0.16	-0.25	-0.28	-1.03	-1.12	-0.07	
S.D.	0.25	0.25	0.17	0.19	0.09	0.09	0.37	0.38	0.01	

Table S 3 ERF, ERF_ts, multimodel means and standard error for the chemically reactive gases.

ERF	**CH4**		**HC**		**N2O**		**NTCF**		**O3**		**NOx**		**VOC**	
Wm^{-2}	**ERF**	**ERF_ts**	**ERF**	**ERF_ts**	**ERF**	**ERF_ts**	**ERF**	**ERF_ts**	**ERF**	**ERF_ts**	**ERF**	**ERF_ts**	**ERF**	**ERF_ts**
CNRM-ESM2	0.44	0.46	-0.10	-0.10	0.32	0.33	-0.74	-0.79						
UKESM1	0.97	1.00	-0.18	-0.19	0.25		-1.03	-1.03	0.21	0.22	0.03	0.04	0.33	0.34
MRI-ESM2	0.70	0.73	0.31	0.31	0.19		-1.08		0.06	0.15	-0.02	-0.02	-0.03	-0.03
BCC-ESM1	0.68	0.72							0.21	0.24	0.12	0.15	-0.04	-0.04
MIROC6							-0.85	-0.83						
NorESM2	0.37	0.39			0.23	0.24								
GFDL-ESM4	0.68	0.70	0.06	0.08			-0.51	-0.55	0.27	0.29	0.14	0.16	0.08	-0.08
GISS-E2-1	0.78	0.80	0.28	0.29	0.20	0.20	-0.92	-0.98	0.23	0.23	0.16	0.16	0.22	0.22
CESM2-WACCM	0.72	0.76	0.34	0.38	0.39	0.40	-0.89	-0.89			0.40	0.44	0.00	0.00
IPSL-INCA														
MultiModel Mean	0.67	0.69	0.12	0.13	0.26	0.29	-0.86	-0.85	0.20	0.23	0.14	0.15	0.09	0.07
S. D.	0.17	0.18	0.21	0.22	0.07	0.08	0.18	0.15	0.07	0.05	0.13	0.14	0.14	0.15

In Table S4 the mean ERF per emissions or concentrations is given for each experiment.

Table S 4 Table of ERF/emissions or concentrations. Emissions for NOx are scaled to Tg of NO2

ERF/emission or concentration	BC (Wm^{-2}/Tg)	SO2 (Wm^{-2}/Tg)	OC (Wm^{-2}/Tg)	NH3 (Wm^{-2}/Tg)	NOx (scaled to Wm^{-2}/Tg NO2)	CH4 (Wm^{-2}/ppb)	HC (Wm^{-2}/ppb)	N2O (Wm^{-2}/ppb)

	0.0212	-0.0094	-0.0147	-0.0013	0.0010	0.0007	0.1200	0.0048

S3 Kernel Breakdown of atmospheric adjustments for each experiment

The full breakdowns of the rapid adjustments as calculated from the kernels is shown for each of the models and experiments where the relevant data was available and shows the differences in models for how the rapid adjustments from different processes contributed to the overall rapid adjustment.

Table S5a Adjustments for piClim-aer experiment

piClim-aer	CNRM-ESM2	UKESM1	MRI-ESM2	BCC-ESM1	MIROC6	NorESM2	GFDL-ESM4	GISS-E2-1
albedo	-0.017	-0.049	-0.009	-0.095	-0.026	-0.015	-0.044	0.003
cloud	-0.661	-0.915	-0.842	-0.900	-0.945	-1.093	-0.452	-0.581
W.V.	-0.055	0.017	0.169	-0.008	-0.085	0.029	0.094	-0.046
T_trop	0.107	0.023	-0.243	0.092	0.183	0.038	-0.138	0.137
T_strat	-0.015	-0.006	-0.014	-0.038	0.010	-0.054	-0.027	-0.038
T_surface	0.054	0.049	0.032	0.075	0.059	0.001	0.035	0.052

Table S5b Adjustments for piClim-BC experiment

piClim-BC	CNRM-ESM2	UKESM1	MRI-ESM2	BCC-ESM1	MIROC6	NorESM2	GISS-E2-1
albedo	0.003	-0.013	0.067	0.015	-0.002	0.076	0.046
cloud	-0.010	-0.013	0.163	0.053	-0.282	-0.067	-0.184
W.V.	0.060	0.057	0.329	0.076	-0.042	0.097	0.038
T_trop	-0.088	-0.137	-0.509	-0.131	0.033	-0.137	-0.051
T_strat	-0.003	0.043	0.021	-0.004	-0.008	-0.025	-0.003
T_surface	0.001	0.005	-0.022	-0.002	0.021	-0.003	0.003

Table S5c Adjustments for piClim-OC experiment

piClim-OC	CNRM-ESM2	UKESM	MRI	MIROC6	NorESM2	GISS-E2-1
albedo	0.008	-0.015	-0.006	-0.017	0.002	0.001
cloud	-0.083	0.052	-0.129	-0.087	-0.100	-0.290
W.V.	0.000	-0.018	-0.009	-0.004	-0.008	-0.054
T_trop	0.025	0.023	-0.016	0.029	0.066	0.057
T_strat	-0.019	-0.003	-0.010	-0.008	-0.016	-0.015
T_surface	0.011	0.015	0.009	0.035	0.010	0.012

Table S5d Adjustments for piClim-SO2 experiment

piClim-SO2	CNRM-ESM2	UKESM1	MRI-ESM2	BCC-ESM1	MIROC6	NorESM2	GISS-E2-1
albedo	0.01	-0.03	-0.04	-0.10	-0.02	-0.09	-0.04
cloud	-0.49	-0.79	-0.73	-0.43	-0.40	-0.96	-0.02
W.V.	-0.04	-0.10	-0.05	-0.07	-0.06	-0.05	-0.06
T_trop	0.10	0.20	0.08	0.22	0.11	0.16	0.14
T_strat	-0.01	-0.02	-0.02	-0.03	0.00	-0.03	-0.01
T_surface	0.03	0.04	0.06	0.07	0.04	0.01	0.03

Table S5e Adjustments for piClim-CH4 experiment

piClim-CH4	CNRM-ESM2	UKESM1	MRI-ESM2	BCC-ESM1	NorESM2	GFDL-ESM4	GISS-E2-1	CESM2-WACCM
albedo	0.019	0.019	0.013	0.031	0.010	0.014	0.007	0.023
cloud	-0.038	0.242	-0.056	0.008	-0.041	-0.054	0.035	0.045
W.V.	0.071	0.109	0.070	0.055	0.018	0.117	0.021	0.068
T_trop	-0.084	-0.162	-0.138	-0.127	-0.080	-0.147	-0.056	-0.082
T_strat	0.114	0.115	0.124	0.039	0.057	0.109	0.053	0.103
T_surface	-0.017	-0.031	-0.028	-0.046	-0.018	-0.023	-0.019	-0.031

Table S5f Adjustments for piClim-HC experiment

piClim-HC	CNRM-ESM2	UKESM1	MRI-ESM2	GFDL-ESM4	GISS-E2-1	CESM2-WACCM
albedo	0.01	-0.02	0.00	0.00	-0.01	0.01
cloud	-0.05	-0.09	-0.02	-0.03	0.03	0.06
W.V.	-0.02	-0.09	0.02	-0.01	-0.01	0.01
T_trop	0.03	0.10	-0.03	-0.03	-0.01	0.00
T_strat	0.21	0.47	0.16	0.26	0.30	0.16
T_surface	0.00	0.01	0.00	-0.02	-0.01	-0.03

Table S5g Adjustments for piClim-N2O experiment

piClim-NO2	CNRM-ESM2	UKESM1	MRI-ESM2	NorESM2	GISS-E2-1	CESM2-WACCM
albedo	0.021	0.001	0.005	0.003	0.000	0.008
cloud	-0.010	0.047	0.004	0.059	0.026	0.119

W.V.	0.038	-0.002	-0.015	-0.012	-0.006	0.016
T_trop	-0.035	-0.006	-0.022	-0.037	-0.002	-0.014
T_strat	0.094	0.074	0.108	0.003	0.130	0.089
T_surface	-0.016	-0.011	-0.005	-0.014	0.005	-0.016

Table S5h Adjustments for piClim-NOx experiment

piClim-NOx	UKESM1	MRI-ESM2	BCC-ESM1	GFDL-ESM4	GISS-E2-1	CESM2-WACCM
albedo	-0.005	0.018	0.023	0.010	0.003	0.041
cloud	-0.036	-0.041	0.007	-0.065	-0.052	0.104
Spec. Hum.	-0.003	-0.040	0.031	0.029	0.005	0.062
T_trop	0.002	-0.014	-0.063	-0.057	-0.001	-0.056
T_strat	-0.024	-0.161	0.029	0.038	0.056	0.095
T_surface	-0.012	-0.012	-0.026	-0.025	-0.001	-0.030

Table S5i Adjustments for piClim-O3 experiment

piClim-O3	UKESM1	MRI-ESM2	BCC-ESM1	GFDL-ESM4	GISS-E2-1
albedo	0.001	0.002	0.026	0.009	-0.003
cloud	0.091	-0.126	0.096	-0.079	-0.021
W.V.	0.006	0.010	0.054	0.082	-0.004
T_trop	-0.034	-0.062	-0.115	-0.083	-0.021
T_strat	0.009	-0.036	0.047	0.094	0.113
T_surface	-0.016	-0.010	-0.037	-0.015	0.002

Table S5j Adjustments for piClim-VOC experiment

piClim-VOC	UKESM1	MRI-ESM2	BCC-ESM1	GFDL-ESM4	GISS-E2-1	CESM2-WACCM
albedo	0.008	0.006	0.000	0.002	-0.001	0.004
cloud	0.190	-0.147	-0.020	-0.004	-0.001	0.033
W.V.	0.023	0.050	0.022	0.067	0.010	-0.049
T_trop	-0.009	-0.072	-0.046	-0.059	-0.006	0.072
T_strat	0.042	0.054	-0.001	0.024	0.064	0.021
T_surface	-0.006	-0.016	-0.011	-0.011	0.002	0.000

Bar charts showing the atmospheric adjustments calculated from the kernel analysis are included below, showing adjustments for surface albedo, cloud, water vapour, tropospheric temperature, stratospheric temperature, and surface temperature.

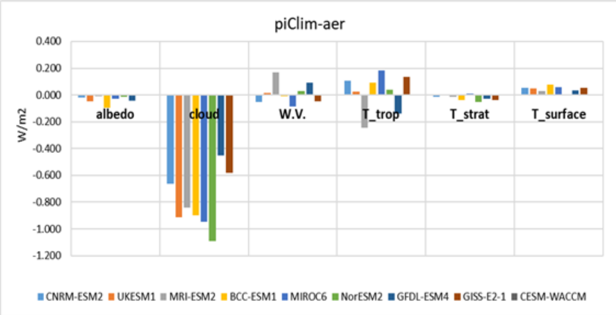
piClim-aer
W/m2
albedo
cloud
W.V.
T_trop
T_strat
T_surface
CNRM-ESM2 UKESM1 MRI-ESM2 BCC-ESM1 MIROC6 NorESM2 GFDL-ESM4 GISS-E2-1 CESM-WACCM

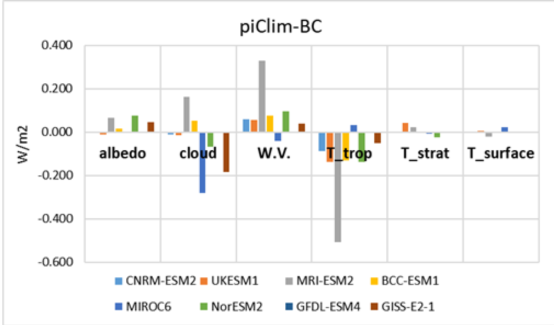
piClim-BC
W/m2
albedo
cloud
W.V.
T_trop
T_strat
T_surface
CNRM-ESM2 UKESM1 MRI-ESM2 BCC-ESM1
MIROC6 NorESM2 GFDL-ESM4 GISS-E2-1

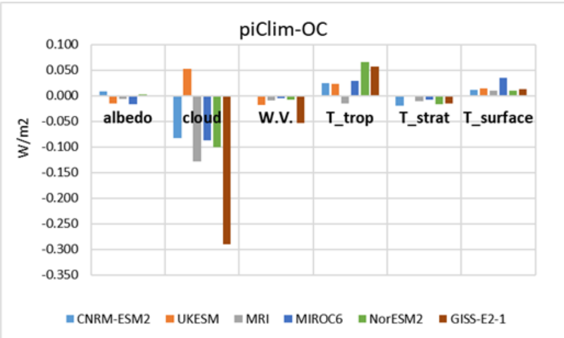
piClim-OC
W/m2
albedo
cloud
W.V.
T_trop
T_strat
T_surface
CNRM-ESM2 UKESM MRI MIROC6 NorESM2 GISS-E2-1

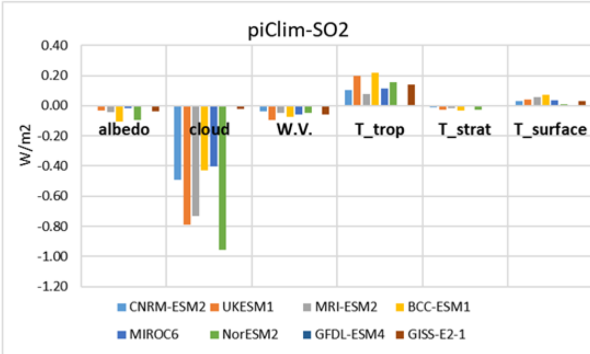
piClim-SO2
W/m2
albedo
cloud
W.V.
T_trop
T_strat
T_surface
CNRM-ESM2 UKESM1 MRI-ESM2 BCC-ESM1
MIROC6 NorESM2 GFDL-ESM4 GISS-E2-1

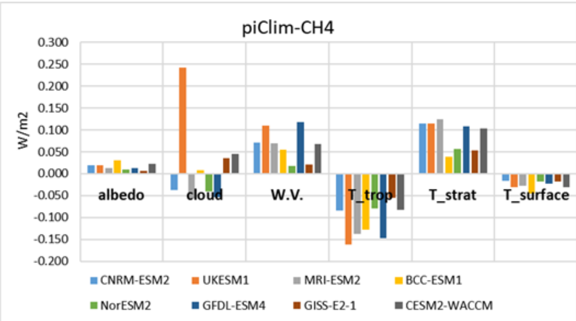
piClim-CH4
W/m2
albedo
cloud
W.V.
T_trop
T_strat
T_surface
CNRM-ESM2 UKESM1 MRI-ESM2 BCC-ESM1
NorESM2 GFDL-ESM4 GISS-E2-1 CESM2-WACCM

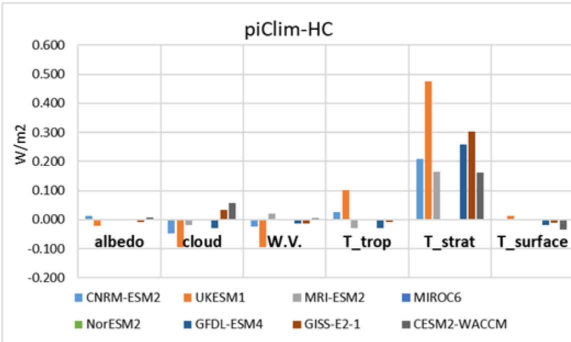
piClim-HC
W/m2
albedo
cloud
W.V.
T_trop
T_strat
T_surface
CNRM-ESM2 UKESM1 MRI-ESM2 MIROC6
NorESM2 GFDL-ESM4 GISS-E2-1 CESM2-WACCM

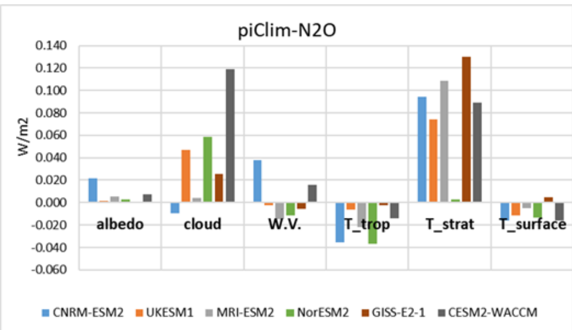
piClim-N2O
W/m2
albedo
cloud
W.V.
T_trop
T_strat
T_surface
CNRM-ESM2 UKESM1 MRI-ESM2 NorESM2 GISS-E2-1 CESM2-WACCM

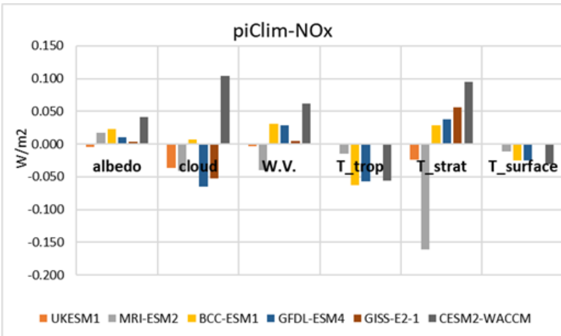
piClim-NOx
W/m2
albedo
cloud
W.V.
T_trop
T_strat
T_surface
UKESM1 MRI-ESM2 BCC-ESM1 GFDL-ESM4 GISS-E2-1 CESM2-WACCM

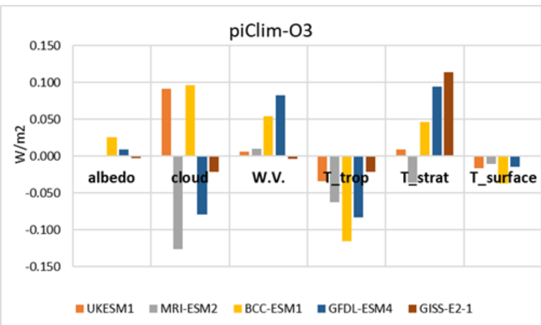
piClim-O3
W/m2
albedo
cloud
W.V.
T_trop
T_strat
T_surface
UKESM1 MRI-ESM2 BCC-ESM1 GFDL-ESM4 GISS-E2-1

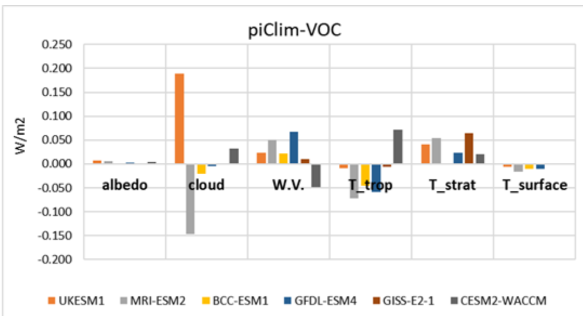
piClim-VOC
W/m2
albedo
cloud
W.V.
T_trop
T_strat
T_surface
UKESM1 MRI-ESM2 BCC-ESM1 GFDL-ESM4 GISS-E2-1 CESM2-WACCM

Figure S 1 Plots showing the breakdown of rapid adjustments for all experiments and models with the appropriate diagnostics

Table S 5 Comparison of IRF and cloud adjustment with Smith et al. (2020) for piClim-aer experiment.

piClim-aer **(Wm^{-2})**	IRF (This work)	IRF (Smith et al., 2020))	IRF Diff	Cloud adj. (This work)	Cloud adj. (Smith et al., 2020)	Cloud adj. Diff	IRF+Cld Adj (this work)	IRF+Cloud Adj. (Smith et al., 2020)	Total Diff	% Diff
CNRM-ESM2-1	-0.15	-0.75	0.60	-0.66	-0.06	-0.60	-0.82	-0.81	-0.01	0.63
GFDL-ESM4	-0.16	-0.37	0.21	-0.45	-0.26	-0.19	-0.61	-0.63	0.02	-2.77
GISS-E2-1-G (p3)	-0.42	-1.00	0.58	-0.60	-0.01	-0.59	-1.02	-1.01	-0.01	1.33
MIROC6	-0.21	-1.13	0.92	-0.95	-0.02	-0.93	-1.16	-1.15	-0.01	0.80
MRI-ESM2-0	-0.30	-0.46	0.16	-0.85	-0.68	-0.17	-1.15	-1.14	-0.01	0.79
NorESM2-LM	-0.11	-1.09	0.98	-1.11	-0.08	-1.03	-1.22	-1.17	-0.05	4.28
UKESM1-0-LL	-0.22	-0.97	0.75	-0.93	-0.18	-0.75	-1.15	-1.15	0.00	0.17
Mean	**-0.23**	**-0.82**	**0.60**	**-0.79**	**-0.18**	**-0.61**	**-1.02**	**-1.01**	**-0.01**	**1.01**

(a)

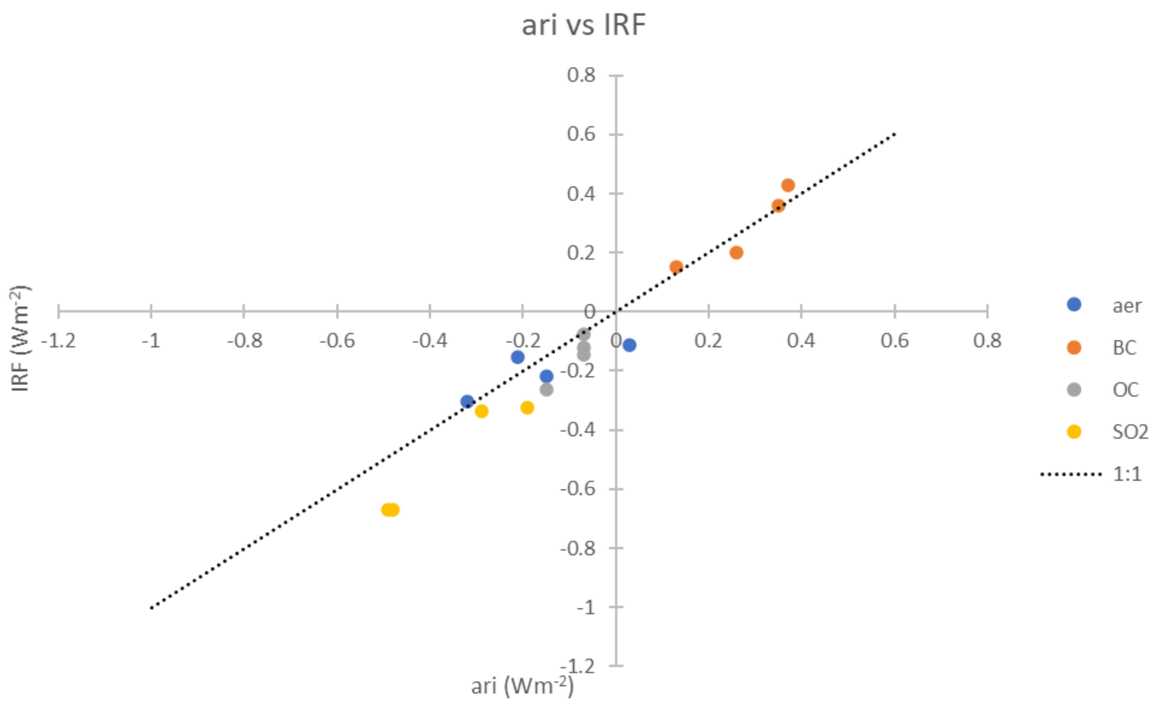

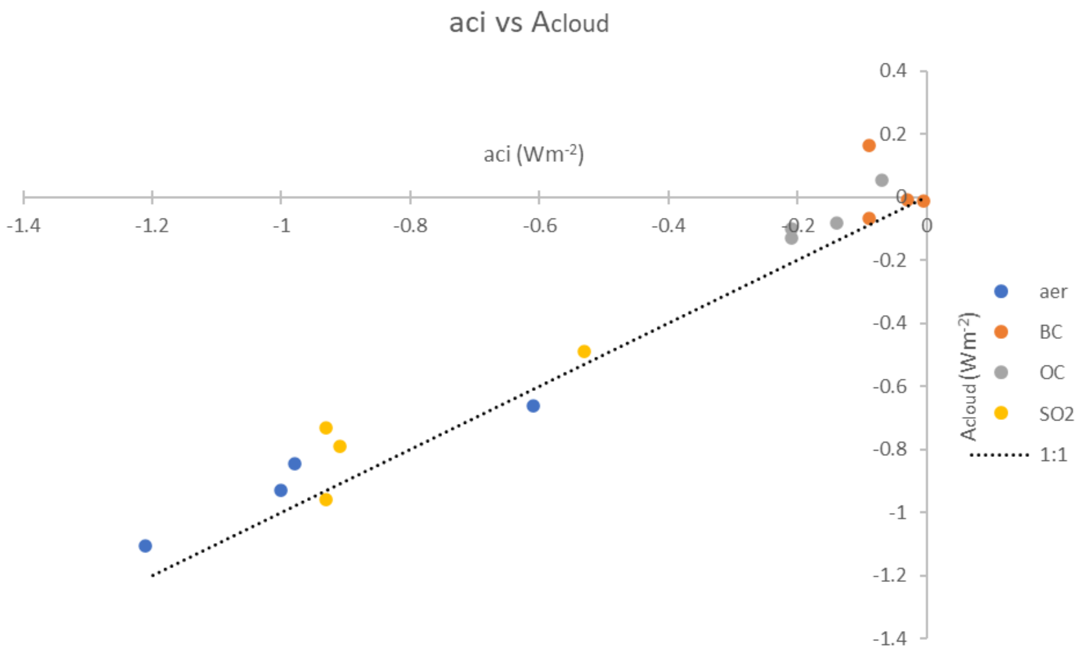

(b)

Figure S 2 Scatter plots comparing direct and indirect aerosol effects from Ghan diagnostics (x-axes) with kernel-derived breakdown (y-axes). Points are from 4 models that included Ghan diagnostics (CNRM-ESM1, UKESM1, MRI-ESM2, NorESM2) (a) Comparison of IRFari with kernel IRF. (b) Comparison of ERFaci with kernel cloud adjustment (Acloud).

S4 AOD scaling

In Fig (S2) we compare the ERF originally calculated from the radiative fluxes for the (piClim-xx –piClim-control) experiments – referred to as Calc ERF to the ERF contributions obtained from using the AOD scaling,

Figure S 3 Comparison of the ERF calculated from radiative fluxes with that from the ERF from AOD-scaled values.

e.g. the BC AOD in the piClim-BC experiment. In general, the change in the single species is responsible for most of the change in the ERF in these experiments, however in the MIROC6 piClim-OC experiment there is a significant contribution from the organic carbon, indicating this is not as clean a method for obtaining the scaling in this case as for the other models and experiments. In the case of NorESM2 for the SO_2 experiment we also have some contribution from the OA, which may be attributable to the way the nucleation scheme works in NorESM2. Their nucleation scheme looks at the combination of H2SO4 and low-volatile organic vapours (precursors of SOA), so changing the SO2 emissions might therefore indirectly change the pathway for the SOA precursors, leading to a shift in how much nucleates and how much condensates. This might lead to a difference in lifetime of SOA (which is part of OM), leading to differences in the OM burden or AOD. (Dirk Olive, pers. Communication).

In Table S6 the ERF per Tg burden is shown for the piClim-BC, piClim-SO2 and piClim-OC experiments.

Table S 6 Table of ERF/burden for individual aerosol experiments

ERF/burden (Wm^{-2} Tg^{-1})	CNRM-ESM2	MIROC6	NorESM2	UKESM1	GISS-E2-1	MRI-ESM2	BCC-ESM1	IPSL-INCA
piClim-BC	1.43	-2.49	2.38	4.07	0.92	1.74	1.63	0.90
piClim-OC	-0.68	-0.67	-0.55	-0.45	-1.42	-1.02		-0.35
piClim-SO2	-1.12	-0.93	-1.17	-1.34	-1.01	-1.47	-1.33	-0.64

S5 Detailed plot of the atmospheric adjustments for the piClim-CH4 model results

The rapid adjustments for the CH4 experiment are broken down to show the model differences and the contributions of the individual rapid adjustments to the overall rapid adjustment contribution to the ERF.

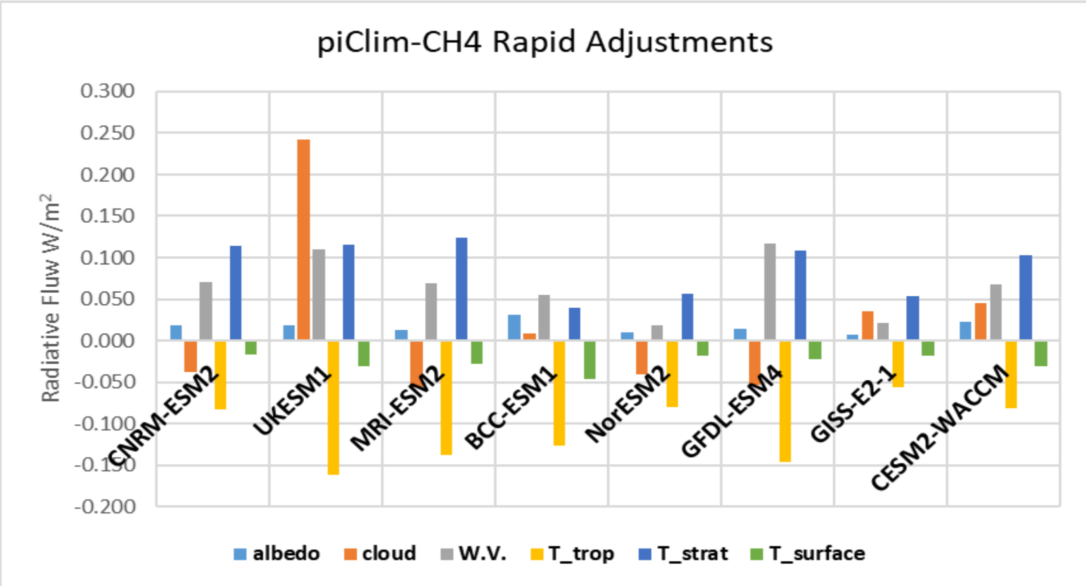

Figure S 4 Plots showing the rapid adjustments for the piClim-CH4 experiments

S5 Plots of the Ghan Calculations

We also plotted the breakdown of the ERF into the ERFari, ERFcloud and the ERFcs,af (clear sky, no aerosol) for models with the appropriate diagnostics, shown in Fig. S4 below.

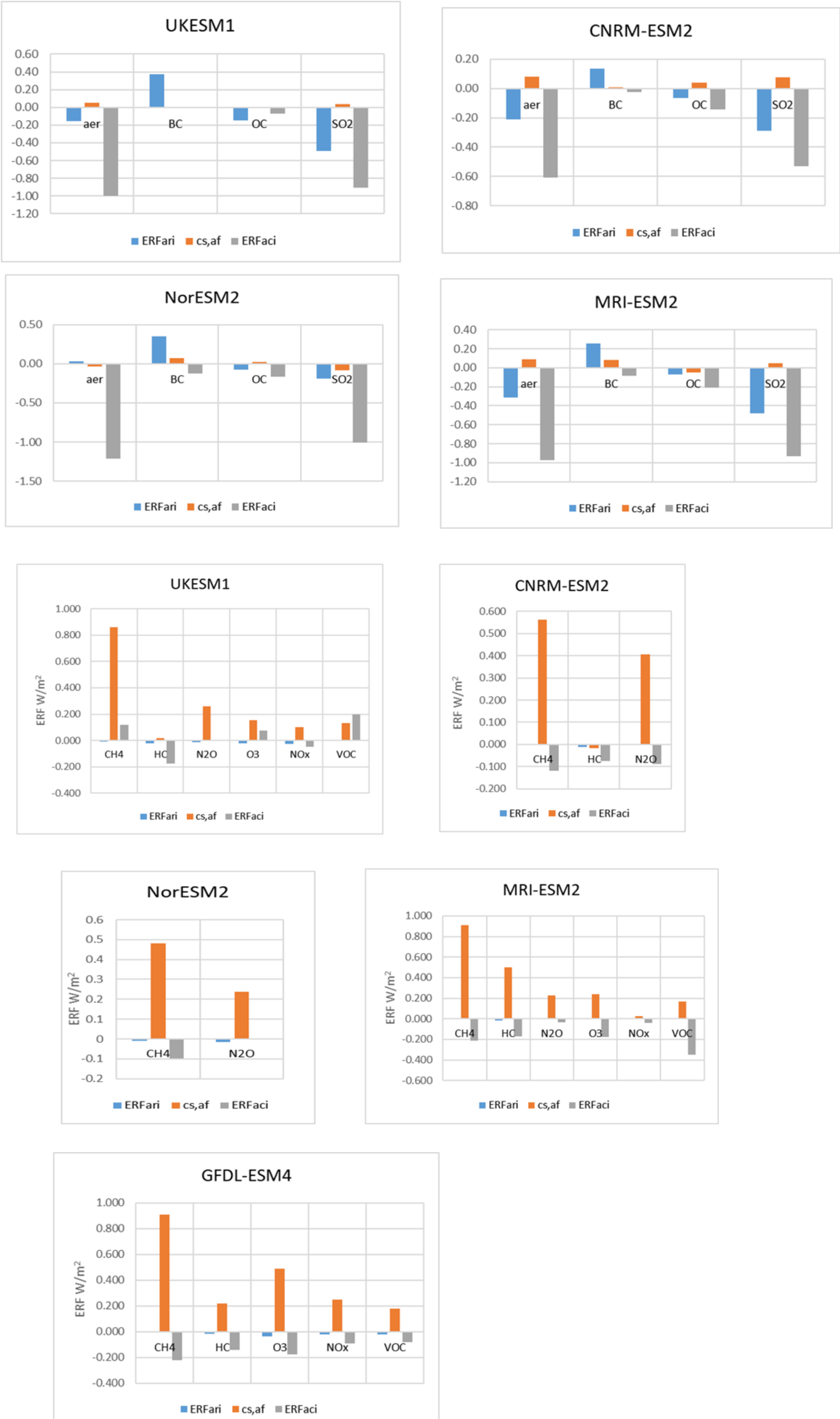

Figure S 5 Breakdown of the ERFs using the double-call method, showing IRFari, ERFcs,af and ERFaci

S6 Experiments using NorESM2 to examine adding 2014 aerosols to an atmosphere with 2014 oxidants.

The following sensitivity experiments were done with the NorESM2 aerosol scheme. To study the effect of SO_2 emissions, we have done a few extra simulations in addition to piClim-control and piClim-SO2 : two additional experiments which we called piClim-oxid and piClim-oxidSO2.

These experiments are :

(1) piClim-control : SO_2 emissions are 1850, oxidants are 1850

(2) piClim-SO_2 : SO_2 emissions are 2014, oxidants are 1850

(3) piClim-oxid : SO_2 emissions are 1850, oxidants are 2014

(4) piClim-oxid+SO_2 : SO_2 emissions are 2014, oxidants are 2014

The standard results in this paper compare (2) with (1) : this gives ERF = -1.303 W/m^2 (N.B the calculations here were done over 25 years, not 30 years as in the rest of the paper). It reflects the impact of adding SO_2 emissions in a clean pre-industrial atmosphere (both (1) and (2) have the oxidants on 1850 levels, as if NOx, CO, VOC, ... emissions are all 1850).

However, if we compare (4) with (3) : this gives -1.479 W/m^2. It is the impact of adding SO_2 emissions, already in a polluted atmosphere where NOx, CO, VOC, ... emissions are at 2014 levels, and therefore high oxidant values.

It shows that we have differences of the order of 13% : ERF = -1.303 W/m^2 compared to -1.479 W/m2.

Similar experiments for all aerosols together result in the following :

(1) piClim-control : aerosol emissions are 1850, oxidants are 1850

(2) piClim-aer : aerosol emissions are 2014, oxidants are 1850

(3) piClim-oxid : aerosol emissions are 1850, oxidants are 2014

(4) piClim-oxid+aer : aerosol emissions are 2014, oxidants are 2014

Comparing here (2) with (1) gives ERF = -1.214 W/m^2 and comparing (4) with (3) gives ERF = -1.458 W/m^2. This gives a difference of around 20%.

This result is only obtained in a simplified setup (prescribed oxidants), but it might give an indication of how the "chemical climate" affects the result.

The climate conditions (different temperature and deposition rates in 1850 and 2014) are of course not covered by the above experiment. It remains in an 1850 climate.

Finally, the impact of large emission reductions (like 100% for SO_2) can show a different sensitivity than smaller mitigation-type reduction sizes due to non-linearity.

(D. Olivie, pers. Comm).

S7 **Breakdown of Ozone changes**

Table S **7** Column ozone, and ozone changes resulting from changes concentrations (CH_4, N_2O, HC) or emissions (NOX, VOC, O_3, NTCF) of reactive gases. The multi model mean does not include the results for CNRM-ESM2 for tropospheric ozone.

Experiment	CNRM-ESM2		UKSM1		MRI-ESM2		BCC-ESM1		GFDL-ESM4		GISS-E2		CESM2-WACCM		Multi-model	
	trop	strat	trop	strat	trop	Strat	trop	strat	trop	strat	trop	strat	trop	strat	trop	strat
Control DU		303.0 ±0.2	25.71 ±0.06	313.2 ±0.6	19.88 ±0.04	294.8 ±0.4	23.20 ±0.03		20.15 ±0.02	267.0 ±0.2	20.45 ±0.04	258.5 ±0.1	20.33 ±0.04	260.3 ±0.2	22.3 ±2.60	283 ±20
CH4 DU		+6.1±0.3	3.02 ±0.08	+2.0 ±0.6	+2.48 ±0.04	+2.9 ±0.5	+2.42 ±0.03		2.50 ±0.04	+2.1 ±0.2	2.17 ±0.05	+5.3 ±0.2	+3.15 ±0.04	+2.9±0.2	+2.6 ±0.3	+4 ±2
NOx DU			5.20 ±0.08	+4.6 ±0.6	+4.09 ±0.05	+10.5 ±0.5	7.23 ±0.03		6.61 ±0.03	+1.1 ±0.2	9.19 ±0.05	+1.0 ±0.2	+6.97 ±0.04	+0.1 ±0.2	+6.5 ±1.6	+3 ±3
VOC DU			1.47 ±0.08	+1.6 ±0.6	+1.99 ±0.05	+2.0 ±0.5	0.79 ±0.03		1.94 ±0.03	+2.5 ±0.2	1.90 ±0.05	-1.9 ±0.3	+1.57 ±0.05	+2.0 ±0.2	+1.6 ±0.4	+1 ±1
O3 DU			6.86 ±0.08	+5.1 ±0.6	+7.51 ±0.04	7.2 ±0.5	8.52 ±0.03		9.46 ±0.03	+2.8 ±0.2	11.38 ±0.06	-0.6 ±0.3			+8.7 ±1.6	+4 ±3
N2O DU		-6.7 ±0.3	0.16 ± 0.08	-3.1 ±0.6	--0.05 ±0.04	-4.7 ±0.5					0.23 ±0.05	-7.6 ±0.2	+0.41 ±0.04	-4.5 ±0.2	+0.2 ±0.2	-5 ±1
HC DU		-23.4 ±0.8	-2.12± 0.08	-38.2 ±0.6	-0.41 ±0.05	-13.4 ±0.5			-1.51 ±0.0	-23.3 ±0.2	-2.54 ±0.05	-24.2 ±0.2	-0.61 ±0.06	-22.7 ±0.4	-1.4 ±0.8	-23 ±8

Table S 8 Percentage change in total aerosol mass (sulphate, nitrate and secondary organic) from the reactive gas experiments.

Experiment	UKESM	MRI-ESM2	BCC-ESM2	GFDL-ESM4			GISS-E2			CESM2-WACCM	
	SO4	SO4	SO4	SO4	NO3	SOA	SO4	NO3	SOA	SO4	SOA
CH4	-2	+2	+1	+6	0	0	-1	-11	+1	-1	-1
NOx	-2	0	+9	-8	+200	+1	-19	+120	+19	+2	-10
VOC	-3	+1	0	+4	-5	+8	-2	0	+1	-2	+34
O3	-4	+1	+10	-3	+190	+7	-21	+130	+21		
N2O	+1	+1					+1	+7	+1	+1	+1
HC	+2	+1		+1	0	+1	+1	-11	+1	-1	+1

S8 Methane Lifetime

Table S 9 Methane lifetime (years), and change due to each experiment (%). Multi-model mean and standard deviation. Lifetimes assume a soil loss of 120 years. Stratospheric loss is included in the model calculations.

Experiment	UKESM1	CESM2-WACCM	GFDL-ESM4	BCC	GISS-E2	MRI-ESM2	Multi-model
Control years	8.0	8.7	9.6	6.3	13.4	10.1	10.0 ±1.9
CH4 %	+22	+22	+21	+26	+18	+22	22±3
NOx %	-25	-35	-33		-46	-26	-33±8
VOC %	+11		+15		+27	+21	+19±6
O3 %	-19		-24		-40	-20	-16±9
HC %	-4.9		-7.5		-0.6	-2.4	-3.7 ±2.4
N2O	-1.2	-2.8			-3.9	-1.3	-2.0 ±1.1

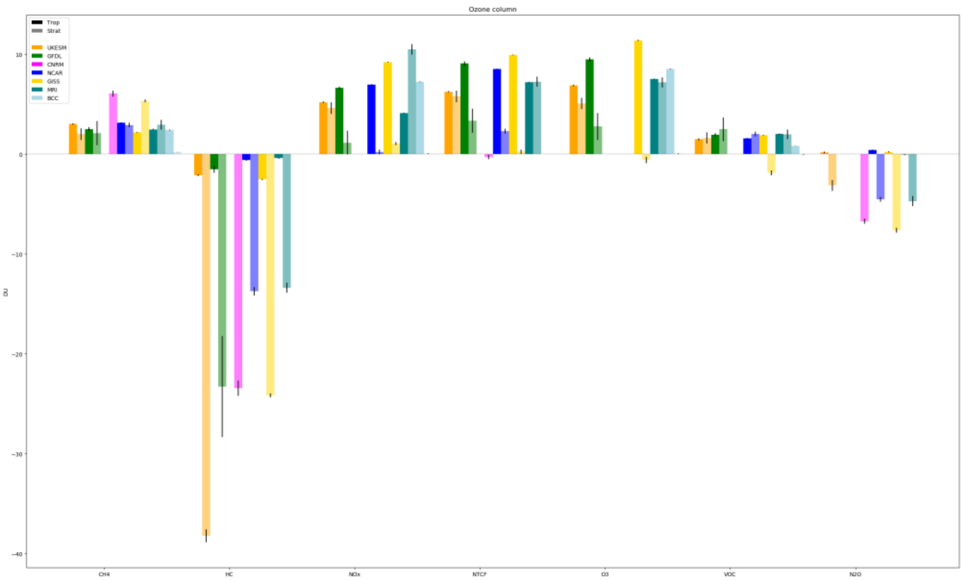

Figure S 6 Ozone column values for the troposphere and stratosphere for the reactive greenhouse gas experiments

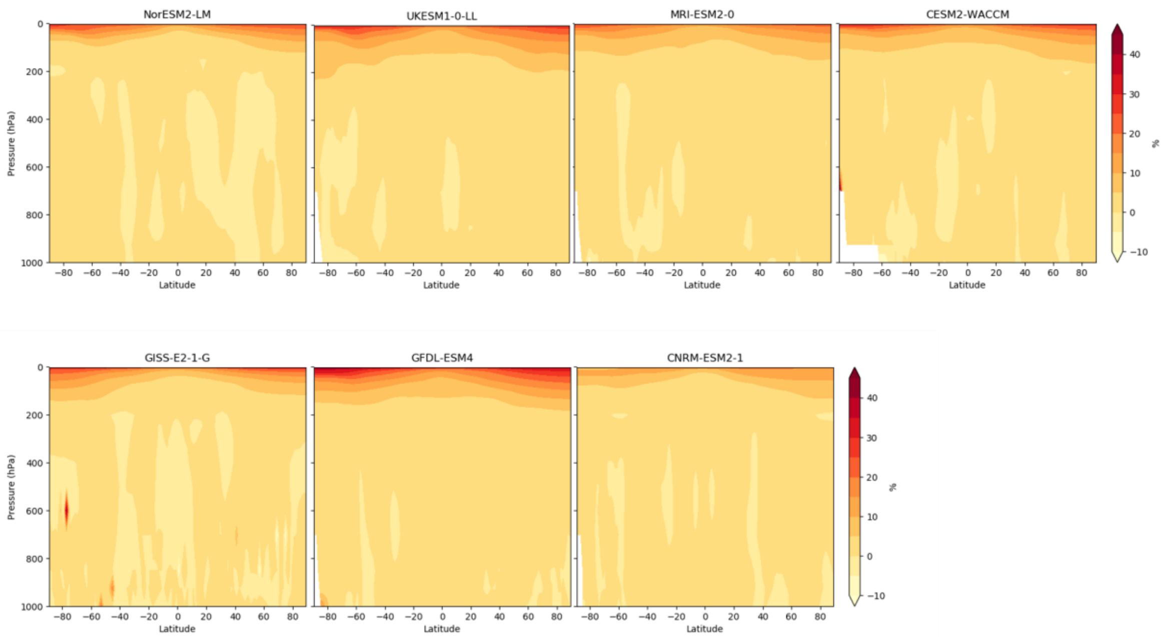

Figure S 7 Percentage changes in water vapour from the piClim-CH4 experiments.

Abdul-Razzak, H., and Ghan, S. J.: A parameterization of aerosol activation: 2. Multiple aerosol types, Journal of Geophysical Research: Atmospheres, 105, 6837-6844, 10.1029/1999jd901161, 2000.

Archibald, A. T., O'Connor, F. M., Abraham, N. L., Archer-Nicholls, S., Chipperfield, M. P., Dalvi, M., Folberth, G. A., Dennison, F., Dhomse, S. S., Griffiths, P. T., Hardacre, C., Hewitt, A. J., Hill, R., Johnson, C. E., Keeble, J., Köhler, M. O., Morgenstern, O., Mulchay, J. P., Ordóñez, C., Pope, R. J., Rumbold, S., Russo, M. R., Savage, N., Sellar, A., Stringer, M., Turnock, S., Wild, O., and Zeng, G.: Description and evaluation of the UKCA stratosphere-troposphere chemistry scheme (StratTrop vn 1.0) implemented in UKESM1, Geosci. Model Dev. Discuss., 2019, 1-82, 10.5194/gmd-2019-246, 2020.

Balkanski, Y., Myhre, G., Gauss, M., Rädel, G., Highwood, E. J., and Shine, K. P.: Direct radiative effect of aerosols emitted by transport: from road, shipping and aviation, Atmos. Chem. Phys., 10, 4477-4489, 10.5194/acp-10-4477-2010, 2010.

Bauer, S. E., Tsigaridis, K., Faluvegi, G., Kelley, M., Lo, K. K., Miller, R. L., Nazarenko, L., Schmidt, G. A., and Wu, J.: Historical (1850–2014) Aerosol Evolution and Role on Climate Forcing Using the GISS ModelE2.1 Contribution to CMIP6, Journal of Advances in Modeling Earth Systems, 12, e2019MS001978, 10.1029/2019ms001978, 2020.

Checa-Garcia, R., Hegglin, M. I., Kinnison, D., Plummer, D. A., and Shine, K. P.: Historical Tropospheric and Stratospheric Ozone Radiative Forcing Using the CMIP6 Database, Geophysical Research Letters, 45, 3264-3273, 10.1002/2017gl076770, 2018.

Danabasoghu, G.: NCAR CESM2-WACCM model output prepared for CMIP6 CMIP historical, https://doi.org/10.22033/ESGF/CMIP6.10071, https://doi.org/10.22033/ESGF/CMIP6.10071, 2019.

Danabasoglu, G.: NCAR CESM2-WACCM model output prepared for CMIP6 ScenarioMIP, https://doi.org/10.22033/ESGF/CMIP6.10026, http://cera-www.dkrz.de/WDCC/meta/CMIP6/CMIP6.ScenarioMIP.NCAR.CESM2-WACCM, 2019.

Di Biagio, C., Formenti, P., Balkanski, Y., Caponi, L., Cazaunau, M., Pangui, E., Journet, E., Nowak, S., Andreae, M., Kandler, K., Saeed, T., Piketh, S., Seibert, D., Williams, E., and Doussin, J.-F.: Complex refractive indices and single scattering albedo of global dust aerosols in the shortwave spectrum and relationship to iron content and size, Atmospheric Chemistry and Physics Discussions, 1-42, 10.5194/acp-2019-145, 2019.

Dunne, J. P., Horowitz, L. W., Adcroft, A. J., Ginoux, P., Held, I. M., John, J. G., Krasting, J. P., Malyshev, S., Naik, V., Paulot, F., Shevliakova, E., Stock, C. A., Zadeh, N., Balaji, V., Blanton, C., Dunne, K. A., Dupuis, C., Durachta, J., Dussin, R., Gauthier, P. P. G., Griffies, S. M., Guo, H., Hallberg, R. W., Harrison, M., He, J., Hurlin, W., McHugh, C., Menzel, R., Milly, P. C. D., Nikonov, S., Paynter, D. J., Ploshay, J., Radhakrishnan, A., Rand, K., Reichl, B. G., Robinson, T., Schwarzkopf, D. M., Sentman, L. T., Underwood, S., Vahlenkamp, H., Winton, M., Wittenberg, A. T., Wyman, B., Zeng, Y., and Zhao, M.: The GFDL Earth System Model version 4.1 (GFDL-ESM 4.1): Overall coupled model description and simulation characteristics, Journal of Advances in Modeling Earth Systems, n/a, e2019MS002015, 10.1029/2019ms002015, 2020.

Emmons, L. K., Schwantes, R. H., Orlando, J. J., Tyndall, G., Kinnison, D., -F., L. J., Marsh, D., Mills, M., Tilmes, S., Bardeen, C., Buchholz, R. R., Conley, A., Gettelman, A., Garcia, R., Simpson, I., Blake, D. R., Meinardi, S., and Pétron, G.: The Chemistry Mechanism in the Community Earth System Model version 2 (CESM2), J. Advances in Modeling Earth Systems, 12, https://doi.org/10.1029/2019MS001882, 2020.

Gery, M. W., Whitten, G. Z., Killus, J. P., and Dodge, M. C.: A photochemical kinetics mechanism for urban and regional scale computer modeling., Journal of Geophysical Research, 94, 925-956, 1989.

Gettelman, A., Mills, M. J., Kinnison, D. E., Garcia, R. R., Smith, A. K., Marsh, D. R., Tilmes, S., Vitt, F., Bardeen, C. G., McInerny, J., Liu, H. L., Solomon, S. C., Polvani, L. M., Emmons, L. K., Lamarque, J. F., Richter, J. H., Glanville, A. S., Bacmeister, J. T., Phillips, A. S., Neale, R. B., Simpson, I. R., DuVivier, A. K., Hodzic, A., and Randel, W. J.: The Whole Atmosphere Community

Climate Model Version 6 (WACCM6), Journal of Geophysical Research: Atmospheres, n/a, 10.1029/2019JD030943, 2019.

Hauglustaine, D. A., Balkanski, Y., and Schulz, M.: A global model simulation of present and future nitrate aerosols and their direct radiative forcing of climate, Atmos. Chem. Phys., 14, 11031-11063, 10.5194/acp-14-11031-2014, 2014.

Horowitz, L. W., Walters, S., Mauzerall, D. L., Emmons, L. K., Rasch, P. J., Granier, C., Tie, X., Lamarque, J.-F., Schultz, M. G., Tyndall, G. S., Orlando, J. J., and Brasseur, G. P.: A global simulation of tropospheric ozone and related tracers: Description and evaluation of MOZART, version 2, Journal of Geophysical Research: Atmospheres, 108, 10.1029/2002jd002853, 2003.

Horowitz, L. W., Naik, V., Paulot, F., Ginoux, P. A., Dunne, J. P., Mao, J., Schnell, J., Chen, X., He, J., John, J. G., Lin, M., Lin, P., Malyshev, S., Paynter, D., Shevliakova, E., and Zhao, M.: The GFDL Global Atmospheric Chemistry-Climate Model AM4.1: Model Description and Simulation Characteristics, Journal of Advances in Modeling Earth Systems, n/a, e2019MS002032, 10.1029/2019ms002032, 2020.

Jones, A., Roberts, D. L., Woodage, M. J., and Johnson, C. E.: Indirect sulphate aerosol forcing in a climate model with an interactive sulphur cycle, Journal of Geophysical Research: Atmospheres, 106, 20293-20310, 10.1029/2000jd000089, 2001.

Khairoutdinov, M., and Kogan, Y.: A New Cloud Physics Parameterization in a Large-Eddy Simulation Model of Marine Stratocumulus, Monthly Weather Review, 128, 229-243, 10.1175/1520-0493(2000)128<0229:ancppi>2.0.co;2, 2000.

Kirkevåg, A., Grini, A., Olivié, D., Seland, Ø., Alterskjær, K., Hummel, M., Karset, I. H. H., Lewinschal, A., Liu, X., Makkonen, R., Bethke, I., Griesfeller, J., Schulz, M., and Iversen, T.: A production-tagged aerosol module for Earth system models, OsloAero5.3 – extensions and updates for CAM5.3-Oslo, Geosci. Model Dev., 11, 3945-3982, 10.5194/gmd-11-3945-2018, 2018.

Kuhlbrodt, T., Jones, C. G., Sellar, A., Storkey, D., Blockley, E., Stringer, M., Hill, R., Graham, T., Ridley, J., Blaker, A., Calvert, D., Copsey, D., Ellis, R., Hewitt, H., Hyder, P., Ineson, S., Mulcahy, J., Siahaan, A., and Walton, J.: The Low-Resolution Version of HadGEM3 GC3.1: Development and Evaluation for Global Climate, Journal of Advances in Modeling Earth Systems, 10, 2865-2888, 10.1029/2018ms001370, 2018.

Lurton, T., Balkanski, Y., Bastrikov, V., Bekki, S., Bopp, L., Braconnot, P., Brockmann, P., Cadule, P., Contoux, C., Cozic, A., Cugnet, D., Dufresne, J.-L., Éthé, C., Foujols, M.-A., Ghattas, J., Hauglustaine, D., Hu, R.-M., Kageyama, M., Khodri, M., Lebas, N., Levavasseur, G., Marchand, M., Ottlé, C., Peylin, P., Sima, A., Szopa, S., Thiéblemont, R., Vuichard, N., and Boucher, O.: Implementation of the CMIP6 Forcing Data in the IPSL-CM6A-LR Model, Journal of Advances in Modeling Earth Systems, 12, e2019MS001940, 10.1029/2019ms001940, 2020.

Mann, G. W., Carslaw, K. S., Spracklen, D. V., Ridley, D. A., Manktelow, P. T., Chipperfield, M. P., Pickering, S. J., and Johnson, C. E.: Description and evaluation of GLOMAP-mode: a modal global aerosol microphysics model for the UKCA composition-climate model, Geosci. Model Dev., 3, 519-551, 10.5194/gmd-3-519-2010, 2010.

Matthes, K., Funke, B., Andersson, M. E., Barnard, L., Beer, J., Charbonneau, P., Clilverd, M. A., Dudok de Wit, T., Haberreiter, M., Hendry, A., Jackman, C. H., Kretzschmar, M., Kruschke, T., Kunze, M., Langematz, U., Marsh, D. R., Maycock, A. C., Misios, S., Rodger, C. J., Scaife, A. A., Seppälä, A., Shangguan, M., Sinnhuber, M., Tourpali, K., Usoskin, I., van de Kamp, M., Verronen, P. T., and Versick, S.: Solar forcing for CMIP6 (v3.2), Geosci. Model Dev., 10, 2247-2302, 10.5194/gmd-10-2247-2017, 2017.

Michou, M., Nabat, P., and Saint-Martin, D.: Development and basic evaluation of a prognostic aerosol scheme (v1) in the CNRM Climate Model CNRM-CM6, Geosci. Model Dev., 8, 501-531, 10.5194/gmd-8-501-2015, 2015.

Morgenstern, O., Braesicke, P., O'Connor, F. M., Bushell, A. C., Johnson, C. E., Osprey, S. M., and Pyle, J. A.: Evaluation of the new UKCA climate-composition model – Part 1: The stratosphere, Geosci. Model Dev., 2, 43-57, 10.5194/gmd-2-43-2009, 2009.

Mulcahy, J. P., Jones, C., Sellar, A., Johnson, B., Boutle, I. A., Jones, A., Andrews, T., Rumbold, S. T., Mollard, J., Bellouin, N., Johnson, C. E., Williams, K. D., Grosvenor, D. P., and McCoy, D. T.: Improved Aerosol Processes and Effective Radiative Forcing in HadGEM3 and UKESM1, Journal of Advances in Modeling Earth Systems, 10, 2786-2805, 10.1029/2018ms001464, 2018.

Mulcahy, J. P., Johnson, C., Jones, C. G., Povey, A. C., Scott, C. E., Sellar, A., Turnock, S. T., Woodhouse, M. T., Abraham, N. L., Andrews, M. B., Bellouin, N., Browse, J., Carslaw, K. S., Dalvi, M., Folberth, G. A., Glover, M., Grosvenor, D., Hardacre, C., Hill, R., Johnson, B., Jones, A., Kipling, Z., Mann, G., Mollard, J., O'Connor, F. M., Palmieri, J., Reddington, C., Rumbold, S. T., Richardson, M., Schutgens, N. A. J., Stier, P., Stringer, M., Tang, Y., Walton, J., Woodward, S., and Yool, A.: Description and evaluation of aerosol in UKESM1 and HadGEM3-GC3.1 CMIP6 historical simulations, Geosci. Model Dev. Discuss., 2020, 1-59, 10.5194/gmd-2019-357, 2020.

O'Connor, F. M., Johnson, C. E., Morgenstern, O., Abraham, N. L., Braesicke, P., Dalvi, M., Folberth, G. A., Sanderson, M. G., Telford, P. J., Voulgarakis, A., Young, P. J., Zeng, G., Collins, W. J., and Pyle, J. A.: Evaluation of the new UKCA climate-composition model – Part 2: The Troposphere, Geosci. Model Dev., 7, 41-91, 10.5194/gmd-7-41-2014, 2014.

Oshima, N., Yukimoto, S., Deushi, M., Koshiro, T., Kawai, H., Tanaka, T. Y., and Yoshida, K.: Global and Arctic effective radiative forcing of anthropogenic gases and aerosols in MRI-ESM2.0, Prog. Earth. Planet. Sci, 7, 38, https://doi.org/10.1186/s40645-020-00348-w, 2020.

Séférian, R., Nabat, P., Michou, M., Saint-Martin, D., Voldoire, A., Colin, J., Decharme, B., Delire, C., Berthet, S., Chevallier, M., Sénési, S., Franchisteguy, L., Vial, J., Mallet, M., Joetzjer, E., Geoffroy, O., Guérémy, J.-F., Moine, M.-P., Msadek, R., Ribes, A., Rocher, M., Roehrig, R., Salas-y-Mélia, D., Sanchez, E., Terray, L., Valcke, S., Waldman, R., Aumont, O., Bopp, L., Deshayes, J., Éthé, C., and Madec, G.: Evaluation of CNRM Earth-System model, CNRM-ESM 2-1: role of Earth system processes in present-day and future climate, Journal of Advances in Modeling Earth Systems, n/a, 10.1029/2019ms001791.

Séférian, R., Delire, C., Decharme, B., Voldoire, A., Salas Y Melia, D., Chevallier, M., Saint-Martin, D., Aumont, O., Calvet, J.-C., Carrer, D., Douville, H., Franchistéguy, L., Joetzjer, E., and Sénési, S.: Development and evaluation of CNRM Earth system model – CNRM-ESM1, Geoscientific Model Development, 9, 1423-1453, 10.5194/gmd-9-1423-2016, 2016.

Sellar, A. A., Jones, C. G., Mulcahy, J., Tang, Y., Yool, A., Wiltshire, A., O'Connor, F. M., Stringer, M., Hill, R., Palmieri, J., Woodward, S., de Mora, L., Kuhlbrodt, T., Rumbold, S., Kelley, D. I., Ellis, R., Johnson, C. E., Walton, J., Abraham, N. L., Andrews, M. B., Andrews, T., Archibald, A. T., Berthou, S., Burke, E., Blockley, E., Carslaw, K., Dalvi, M., Edwards, J., Folberth, G. A., Gedney, N., Griffiths, P. T., Harper, A. B., Hendry, M. A., Hewitt, A. J., Johnson, B., Jones, A., Jones, C. D., Keeble, J., Liddicoat, S., Morgenstern, O., Parker, R. J., Predoi, V., Robertson, E., Siahaan, A., Smith, R. S., Swaminathan, R., Woodhouse, M. T., Zeng, G., and Zerroukat, M.: UKESM1: Description and evaluation of the UK Earth System Model, Journal of Advances in Modeling Earth Systems, n/a, 10.1029/2019ms001739.

Sellar, A. A., Jones, C. G., Mulcahy, J., Tang, Y., Yool, A., Wiltshire, A., O'Connor, F. M., Stringer, M., Hill, R., Palmieri, J., Woodward, S., de Mora, L., Kuhlbrodt, T., Rumbold, S., Kelley, D. I., Ellis, R., Johnson, C. E., Walton, J., Abraham, N. L., Andrews, M. B., Andrews, T., Archibald, A. T., Berthou, S., Burke, E., Blockley, E., Carslaw, K., Dalvi, M., Edwards, J., Folberth, G. A., Gedney, N., Griffiths, P. T., Harper, A. B., Hendry, M. A., Hewitt, A. J., Johnson, B., Jones, A., Jones, C. D., Keeble, J., Liddicoat, S., Morgenstern, O., Parker, R. J., Predoi, V., Robertson, E., Siahaan, A., Smith, R. S., Swaminathan, R., Woodhouse, M. T., Zeng, G., and Zerroukat, M.: UKESM1: Description and evaluation of the UK Earth System Model, Journal of Advances in Modeling Earth Systems, n/a, 10.1029/2019ms001739, 2020.

Shindell, D. T., Grenfell, J. L., Rind, D., Grewe, V., and Price, C.: Chemistry-climate interactions in the Goddard Institute for Space Studies general circulation model: 1. Tropospheric chemistry model description and evaluation, Journal of Geophysical Research: Atmospheres, 106, 8047-8075, 10.1029/2000jd900704, 2001.

Shindell, D. T., Faluvegi, G., and Bell, N.: Preindustrial-to-present-day radiative forcing by tropospheric ozone from improved simulations with the GISS chemistry-climate GCM, Atmos. Chem. Phys., 3, 1675-1702, 10.5194/acp-3-1675-2003, 2003.

Shindell, D. T., Faluvegi, G., Unger, N., Aguilar, E., Schmidt, G. A., Koch, D. M., Bauer, S. E., and Miller, R. L.: Simulations of preindustrial, present-day, and 2100 conditions in the NASA GISS composition and climate model G-PUCCINI, Atmos. Chem. Phys., 6, 4427-4459, 10.5194/acp-6-4427-2006, 2006.

Smith, C. J., Kramer, R. J., Myhre, G., Alterskjær, K., Collins, W., Sima, A., Boucher, O., Dufresne, J. L., Nabat, P., Michou, M., Yukimoto, S., Cole, J., Paynter, D., Shiogama, H., O'Connor, F. M., Robertson, E., Wiltshire, A., Andrews, T., Hannay, C., Miller, R., Nazarenko, L., Kirkevåg, A., Olivié, D., Fiedler, S., Pincus, R., and Forster, P. M.: Effective radiative forcing and adjustments in CMIP6 models, Atmos. Chem. Phys., 20, 9591-9618, 10.5194/acp-20-9591-2020, 2020.

Takemura, T., Nozawa, T., Emori, S., Nakajima, T. Y., and Nakajima, T.: Simulation of climate response to aerosol direct and indirect effects with aerosol transport-radiation model, Journal of Geophysical Research: Atmospheres, 110, 10.1029/2004jd005029, 2005.

Takemura, T., and Suzuki, K.: Weak global warming mitigation by reducing black carbon emissions, Scientific Reports, 9, 4419, 10.1038/s41598-019-41181-6, 2019.

Takemura, T., et al: Development of a global aerosol climate model SPRINTARS, CGER's Supercomputer Monograph Report, 24, 2018.

Tatebe, H., Ogura, T., Nitta, T., Komuro, Y., Ogochi, K., Takemura, T., Sudo, K., Sekiguchi, M., Abe, M., Saito, F., Chikira, M., Watanabe, S., Mori, M., Hirota, N., Kawatani, Y., Mochizuki, T., Yoshimura, K., Takata, K., O'Ishi, R., Yamazaki, D., Suzuki, T., Kurogi, M., Kataoka, T., Watanabe, M., and Kimoto, M.: Description and basic evaluation of simulated mean state, internal variability, and climate sensitivity in MIROC6, Geoscientific Model Development, 12, 2727-2765, http://dx.doi.org/10.5194/gmd-12-2727-2019, 2019.

Tilmes, S., Hodzic, A., Emmons, L. K., Mills, M. J., Gettelman, A., Kinnison, D. E., Park, M., Lamarque, J. F., Vitt, F., Shrivastava, M., Campuzano-Jost, P., Jimenez, J. L., and Liu, X.: Climate Forcing and Trends of Organic Aerosols in the Community Earth System Model (CESM2), Journal of Advances in Modeling Earth Systems, n/a, 10.1029/2019MS001827, 2019.

Walters, D., Baran, A. J., Boutle, I., Brooks, M., Earnshaw, P., Edwards, J., Furtado, K., Hill, P., Lock, A., Manners, J., Morcrette, C., Mulcahy, J., Sanchez, C., Smith, C., Stratton, R., Tennant, W., Tomassini, L., Van Weverberg, K., Vosper, S., Willett, M., Browse, J., Bushell, A., Carslaw, K., Dalvi, M., Essery, R., Gedney, N., Hardiman, S., Johnson, B., Johnson, C., Jones, A., Jones, C., Mann, G., Milton, S., Rumbold, H., Sellar, A., Ujiie, M., Whitall, M., Williams, K., and Zerroukat, M.: The Met Office Unified Model Global Atmosphere 7.0/7.1 and JULES Global Land 7.0 configurations, Geosci. Model Dev., 12, 1909-1963, 10.5194/gmd-12-1909-2019, 2019.

Wang, R., Balkanski, Y., Boucher, O., Ciais, P., Schuster, G. L., Chevallier, F., Samset, B. H., Liu, J., Piao, S., Valari, M., and Tao, S.: Estimation of global black carbon direct radiative forcing and its uncertainty constrained by observations, Journal of Geophysical Research: Atmospheres, 121, 5948-5971, 10.1002/2015jd024326, 2016.

Watanabe, M., Suzuki, T., O'ishi, R., Komuro, Y., Watanabe, S., Emori, S., Takemura, T., Chikira, M., Ogura, T., Sekiguchi, M., Takata, K., Yamazaki, D., Yokohata, T., Nozawa, T., Hasumi, H., Tatebe, H., and Kimoto, M.: Improved Climate Simulation by MIROC5: Mean States, Variability, and Climate Sensitivity, Journal of Climate, 23, 6312-6335, 10.1175/2010jcli3679.1, 2010.

Williams, K. D., Copsey, D., Blockley, E. W., Bodas-Salcedo, A., Calvert, D., Comer, R., Davis, P., Graham, T., Hewitt, H. T., Hill, R., Hyder, P., Ineson, S., Johns, T. C., Keen, A. B., Lee, R. W., Megann, A., Milton, S. F., Rae, J. G. L., Roberts, M. J., Scaife, A. A., Schiemann, R., Storkey, D., Thorpe, L., Watterson, I. G., Walters, D. N., West, A., Wood, R. A., Woollings, T., and Xavier, P. K.: The Met Office Global Coupled Model 3.0 and 3.1 (GC3.0 and GC3.1) Configurations, Journal of Advances in Modeling Earth Systems, 10, 357-380, 10.1002/2017ms001115, 2018.

Woodward, S.: Modeling the atmospheric life cycle and radiative impact of mineral dust in the Hadley Centre climate model, Journal of Geophysical Research: Atmospheres, 106, 18155-18166, 10.1029/2000jd900795, 2001.

Wu, T., Zhang, F., Zhang, J., Jie, W., Zhang, Y., Wu, F., Li, L., Liu, X., Lu, X., Zhang, L., Wang, J., and Hu, A.: Beijing Climate Center Earth System Model version 1 (BCC-ESM1): Model Description and Evaluation, Geosci. Model Dev. , 13, 977-1005, 10.5194/gmd-2019-172, 2020.

Yukimoto, S., Kawai, H., Koshiro, T., Oshima, N., Yoshida, K., Urakawa, S., Tsujino, H., Deushi, M., Tanaka, T., Hosaka, M., Yabu, S., Yoshimura, H., Shindo, E., Mizuta, R., Obata, A., Adachi, Y., and Ishii, M.: The Meteorological Research Institute Earth System Model Version 2.0, MRI-ESM2.0: Description and Basic Evaluation of the Physical Component, J. Meteor. Soc. Japan, 97, 931-965, 10.2151/jmsj.2019-051, 2019.